Modeling reflections with an elastic screen method

Xiao-Bi Xie and Ru-Shan Wu, Institute of Tectonics, University of California, Santa Cruz*

Summary

This paper gives two versions of elastic screen method. The wide angle version has a better accuracy while the small angle approximation is more efficient. The accuracy of the reflectivity is discussed by comparing the analytical results from the screen method and those directly from plane wave reflections. The accuracy of waveform is checked by comparing synthetic seismograms from both screen method and full wave FD method. We also discussed the application of elastic screen method in modeling seismic reflections in 2D or 3D elastic models.

Introduction

For calculating synthetic seismograms, FD and FE algorithms are very flexible. Theoretically, they can be applied to arbitrarily heterogeneous media. However, they are very time consuming. High-frequency asymptotic methods, such as ray based methods, provide high computation efficiency for smooth 3D models. However, they fail in dealing with complicated 3D volume heterogeneities. It is necessary to develop intermediate modeling methods functioning between the full wave equation methods and the high-frequency asymptotic methods. The screen methods have been used to calculate the one-way forward propagations for both acoustic and elastic wave problems (e.g., Martin and Flatté 1988; Wu 1994), and used as back propagator for seismic wave migration in either acoustic or elastic media (e.g., Stoffa et al. 1990, Wu and Xie 1994). The screen methods are based on one-way wave equation that neglects backscattered waves, but correctly handles all the forward multiple-scattering effects. For media where the resonance scattering or reverberations can be neglected, the reflections will be dominated by single back scatterings. In this case, the screen method can also be adopted to calculate reflections. Xie and Wu (1995, 1996) tested the screen approximation for modeling elastic wave reflections. Wu, Huang and Xie (1995), Wu and Huang (1995) tested the method for acoustic reflections. Wu (1996) discussed various approximations for forward and backward scatterings of different wave types.

The screen method has two main advantages. First, it neglects the multiple reflections so that the full wave equation can be replaced by the one-way wave equation, which considerably reduced the CPU time. Second, the screen method manipulates in successive 2D planes instead of the original 3D model, which tremendously reduced the demand for computer memories. These advantages make the complex screen method a very attractive candidate in dealing with complicated 3D models. The trade off of this method is that the reverberations are omitted from the calculation. And, once the small angle approximation is used, large angle scattering is less accurate. In exploration seismology, the reverberations are often omitted or eliminated through the primary data processing, and therefore lack of reverberation in the theory is tolerable for many practical applications. In this paper, we will give both wide angle and a small angle versions of screen method and briefly discuss their accuracies in modeling reflectivity and waveforms.

Brief description of the method

Consider wave incident on an inhomogeneous thin slab with thickness Δz and bounded between z_0 and z_1. The incident wave $\mathbf{u}_0$ will generate backscattered wave $\mathbf{u}_b$ and forward propagated wave $\mathbf{u}_f$. At z_1, the exit side of the slab, the forward propagated field is composed of primary wave and forward scattered P- and S-waves. It can be represented as the superposition of plane P- and S-waves (Xie and Wu, 1995, 1996; Wu, 1996):

$$\mathbf{u}_f(\mathbf{x}_T, z_1) = \frac{1}{4\pi^2}\int d\mathbf{K}_T \left[\mathbf{u}_f^P(\mathbf{K}_T, z_1) + \mathbf{u}_f^S(\mathbf{K}_T, z_1)\right] e^{i\mathbf{K}_T\cdot\mathbf{x}_T} \quad (1)$$

where $\mathbf{K}_T$ is the transverse wavenumber, $\mathbf{x} = \mathbf{x}_T + z\hat{\mathbf{e}}_z$ is the position vector, superscripts P and S denote P- and S-waves, and

$$\mathbf{u}_f^P(\mathbf{K}_T, z_1) = e^{i\gamma_\alpha \Delta z}\left[\mathbf{u}_0^P(\mathbf{K}_T, z_0) + \mathbf{U}_f^{PP}(\mathbf{K}_T, z_0) + \mathbf{U}_f^{SP}(\mathbf{K}_T, z_0)\right] \quad (2)$$

$$\mathbf{u}_f^S(\mathbf{K}_T, z_1) = e^{i\gamma_\beta \Delta z}\left[\mathbf{u}_0^S(\mathbf{K}_T, z_0) + \mathbf{U}_f^{SS}(\mathbf{K}_T, z_0) + \mathbf{U}_f^{PS}(\mathbf{K}_T, z_0)\right] \quad (3)$$

where $k_\alpha = \omega/\alpha$ and $k_\beta = \omega/\beta$ are P and S wavenumbers, γ_α and γ_β are longitudinal components of these wavenumbers. Phase advance operators $e^{i\gamma_\alpha \Delta z}$ and $e^{i\gamma_\beta \Delta z}$ propagate the incident and scattered fields from z_0 to z_1. The reflected wave is composed of reflected

P- and S-waves. At z_0, the reflected wave can be expressed as

$$\mathbf{u}_b(\mathbf{x}_T, z_0) = \frac{1}{4\pi^2}\int d\mathbf{K}_T \left[\mathbf{u}_b^P(\mathbf{K}_T, z_0) + \mathbf{u}_b^S(\mathbf{K}_T, z_0)\right] e^{i\mathbf{K}_T\cdot\mathbf{x}_T} \quad (4)$$

where

$$\mathbf{u}_b^P(\mathbf{K}_T, z_0) = \mathbf{U}_b^{PP}(\mathbf{K}_T, z_0) + \mathbf{U}_b^{SP}(\mathbf{K}_T, z_0) \quad (5)$$

$$\mathbf{u}_b^S(\mathbf{K}_T, z_0) = \mathbf{U}_b^{SS}(\mathbf{K}_T, z_0) + \mathbf{U}_b^{PS}(\mathbf{K}_T, z_0) \quad (6)$$

In the above equations, $\mathbf{U}$ denotes scattered waves. The subscripts f and b denote forward and backward scatterings, respectively. Superscripts PP, PS, SP and SS indicate the scattering between different wave types. Here we will analyze only reflections, i.e., back scatterings. Under wide angle approximation, these scattered waves can be expressed as

$$\mathbf{U}_b^{PP}(\mathbf{K}'_T, \mathbf{K}_T) = \frac{i}{2\gamma'_\alpha}\Delta z k_\alpha^2 u_0^P(\mathbf{K}_T)\hat{k}'_\alpha \quad (7)$$
$$\left\{(\hat{k}_\alpha\cdot\hat{k}'_\alpha)\frac{\delta\rho(\tilde{\mathbf{K}}_T)}{\rho_0} - \frac{\delta\lambda(\tilde{\mathbf{K}}_T)}{\lambda_0+2\mu_0} - (\hat{k}_\alpha\cdot\hat{k}'_\alpha)^2\frac{2\delta\mu(\tilde{\mathbf{K}}_T)}{\mu_0}\right\}\eta_b^{PP}$$

$$\mathbf{U}_b^{PS}(\mathbf{K}'_T, \mathbf{K}_T) = \frac{i}{2\gamma'_\beta}k_\beta^2 u_0^P[\hat{k}_\alpha - \hat{k}'_\beta(\hat{k}_\alpha\cdot\hat{k}'_\beta)]$$
$$\left\{\frac{\delta\rho(\tilde{\mathbf{K}}_T)}{\rho_0} - 2\frac{\beta_0}{\alpha_0}(\hat{k}_\alpha\cdot\hat{k}'_\beta)\frac{\delta\mu(\tilde{\mathbf{K}}_T)}{\mu_0}\right\}\eta_b^{PS} \quad (8)$$

$$\mathbf{U}_b^{SP}(\mathbf{K}'_T, \mathbf{K}_T) = \frac{i}{2\gamma'_\alpha}k_\alpha^2(\mathbf{u}_0^S\cdot\hat{k}'_\alpha)\hat{k}'_\alpha$$
$$\left\{\frac{\delta\rho(\tilde{\mathbf{K}}_T)}{\rho_0} - 2\frac{\beta_0}{\alpha_0}(\hat{k}_\beta\cdot\hat{k}'_\alpha)\frac{\delta\mu(\tilde{\mathbf{K}}_T)}{\mu_0}\right\}\eta_b^{SP} \quad (9)$$

$$\mathbf{U}_b^{SS}(\mathbf{K}'_T, \mathbf{K}_T) = \frac{i}{2\gamma'_\beta}k_\beta^2\left\{[\mathbf{u}_0^S - \hat{k}'_\beta(\mathbf{u}_0^S\cdot\hat{k}'_\beta)]\frac{\delta\rho(\tilde{\mathbf{K}}_T)}{\rho_0}\right\}$$
$$-\left[(\hat{k}_\beta\cdot\hat{k}'_\beta)[\mathbf{u}_0^S - \hat{k}'_\beta(\mathbf{u}_0^S\cdot\hat{k}'_\beta)]\right.$$
$$\left.+(\mathbf{u}_0^S\cdot\hat{k}'_\alpha)(\hat{k}_\beta - \hat{k}'_\beta(\hat{k}_\beta\cdot\hat{k}'_\beta))\right]\left\{\frac{\delta\mu(\tilde{\mathbf{K}}_T)}{\mu_0}\right\}\eta_b^{SS} \quad (10)$$

where $\mathbf{K}_T$ is the incident wavenumber and $\mathbf{K}'_T$ is the scattered wavenumber, $\tilde{\mathbf{K}}_T = \mathbf{K}'_T - \mathbf{K}_T$, η is the modulation factor for different waves. λ, μ and ρ are Lame parameters and density. $\delta\lambda, \delta\mu$ and $\delta\rho$ are their perturbations. Under the small-angle approximation, γ_α and γ'_α can be approximated by k_α, and γ_β and γ'_β by k_β. For backward scattering $(\hat{k}_\alpha\cdot\hat{k}'_\alpha)$, $(\hat{k}_\beta\cdot\hat{k}'_\beta)$, $(\hat{k}_\beta\cdot\hat{k}'_\alpha)$ and $(\hat{k}_\alpha\cdot\hat{k}'_\beta)$ all approach to -1. We obtain the backward scattered waves for small angle approximation

$$\mathbf{U}_b^{PP}(\mathbf{K}'_T, \mathbf{K}_T) = -ik_\alpha\Delta z\,\hat{k}'_\alpha u_0^P(\mathbf{K}_T) \times\left[\frac{\delta\rho(\tilde{\mathbf{K}}_T)}{\rho_0} + \frac{\delta\alpha(\tilde{\mathbf{K}}_T)}{\alpha_0}\right]\eta_b^{PP} \quad (11)$$

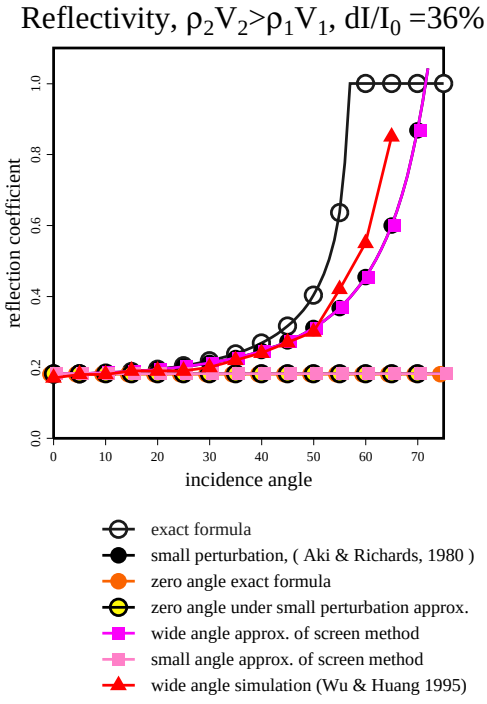

Figure 1: Reflection coefficients from different approximations.

$$\mathbf{U}_b^{PS}(\mathbf{K}'_T, \mathbf{K}_T) = -ik_\beta\Delta z\,u_0^P(\mathbf{K}_T)\left[\hat{k}_\alpha - \hat{k}'_\beta(\hat{k}_\alpha\cdot\hat{k}'_\beta)\right] \times\left[\frac{\delta\beta(\tilde{\mathbf{K}}_T)}{\beta_0} - \left(\frac{\beta_0}{\alpha_0}+\frac{1}{2}\right)\frac{\delta\mu(\tilde{\mathbf{K}}_T)}{\mu_0}\right]\eta_b^{PS} \quad (12)$$

$$\mathbf{U}_b^{SP}(\mathbf{K}'_T, \mathbf{K}_T) = -ik_\alpha\Delta z(\mathbf{u}_0^S(\mathbf{K}_T)\cdot\hat{k}'_\alpha)\hat{k}'_\alpha \times\left[\frac{\delta\beta(\tilde{\mathbf{K}}_T)}{\beta_0} - \left(\frac{\beta_0}{\alpha_0}+\frac{1}{2}\right)\frac{\delta\mu(\tilde{\mathbf{K}}_T)}{\mu_0}\right]\eta_b^{SP} \quad (13)$$

$$\mathbf{U}_b^{SS}(\mathbf{K}'_T, \mathbf{K}_T) = ik_\beta\Delta z\left[\mathbf{u}_0^S(\mathbf{K}_T) - \hat{k}'_\beta(\mathbf{u}_0^S(\mathbf{K}_T)\cdot\hat{k}'_\beta)\right] \times\left[\frac{\delta\rho(\tilde{\mathbf{K}}_T)}{\rho_0} + \frac{\delta\beta(\tilde{\mathbf{K}}_T)}{\beta_0}\right]\eta_b^{SS} \quad (14)$$

Accuracies of reflectivities

The reflection coefficients depend on both incident angle and model parameters. Amplitude information sometimes are important in seismic data processing, for example, the AVO analysis. Here, by analizing a special case where plane wave incident on a plane interface, we will examine the reflection coefficients derived from the screen method, and compare them with those directly obtained from plane wave theory. Taking incident P-wave as an example, from equation (4), the reflected P-wave can be expressed as

$$\mathbf{u}_b^P(\mathbf{x}_T, z_0) = \frac{1}{4\pi^2}\int d\mathbf{K}'_T e^{i\mathbf{K}'_T\cdot\mathbf{x}_T}$$

$$\times \frac{1}{4\pi^2} \int d\mathbf{K}_T \mathbf{U}_b^{PP}(\mathbf{K}'_T, \mathbf{K}_T, z_0) \quad (15)$$

Substitute the wide angle approximation equation (7) into the above equation. For plane wave incidence, $u_0^P(\mathbf{K}_T)$ is a Dirac δ function of $\mathbf{K}_T$, and for a horizontal constant velocity layer, the perturbation spectra $\delta\alpha, \delta\lambda$ and $\delta\mu$ are also Dirac δ functions with contributions only at $\mathbf{K}'_T - \mathbf{K}_T = 0$. With these spectra, only reflections with $\mathbf{K}'_T = \mathbf{K}_T$ can be generated and which is the Snell's law. From these wave functions and model spectra, equation (15) can be directly integrated.

$$u_b^P(\mathbf{x}_T, z_0) = \frac{1}{4}\frac{k_\alpha^2}{\gamma_\alpha}\mathbf{u}_0^P \left[(\hat{k}_\alpha \cdot \hat{k}'_\alpha)\frac{\delta\rho}{\rho} + \frac{\delta\lambda}{\lambda_0 + +2\mu_0} - (\hat{k}_\alpha \cdot \hat{k}'_\alpha)^2 \frac{2\delta\mu}{\lambda_0 + 2\mu_0} \right]$$

The P to P reflectivity is

$$R^{PP} = \frac{u_b^P}{u_0^P} = (\frac{1}{2} - 2\beta_0^2 p^2)\frac{\delta\rho}{\rho} + \frac{1}{2\cos^2 i}\frac{\delta\alpha}{\alpha_0} - 4\beta_0^2 p^2 \frac{\delta\beta}{\beta_0} \quad (16)$$

where $p = \sin i/\alpha$ is the ray parameter for the plane wave and i is the P-wave incident angle. If shear modular μ vanishes, the above equation gives reflectivity for acoustic waves under small impedence contrast.

$$R^{ACOUS} = \frac{1}{2}(\frac{\delta\rho}{\rho} + \frac{1}{\cos^2 i}\frac{\delta\alpha}{\alpha_0}) \quad (17)$$

Similarly, for P to S reflection we have

$$R^{PS} = \frac{u_b^S}{u_0^P} = \frac{\alpha_0 p}{2\cos^2 j}\left\{ \left[1 - 2\beta_0^2 p^2 + 2\beta_0^2 \frac{\cos i}{\alpha_0}\frac{\cos j}{\beta_0} \right]\frac{\delta\rho}{\rho} - \left[4\beta_0^2 p^2 - 4\beta_0^2 \frac{\cos i}{\alpha_0}\frac{\cos j}{\beta_0} \right]\frac{\delta\beta}{\beta_0} \right\} \quad (18)$$

where j is S-wave incident angle. Equations (16) and (18) are consistent with the reflectivities given by Aki and Rechards (1980) for interface between two half-spaces having similar properties (small perturbations), i.e., $\delta\rho/\rho$ etc. $\ll 1$.

Substituting equations (11) or (12) into (4), we can obtain reflectivities R^{PP} and R^{PS} for small angle approximation. They are

$$R^{PP} = \frac{\rho_2\alpha_2 - \rho_1\alpha_1}{\rho_2\alpha_2 + \rho_1\alpha_1} \quad (19)$$

$$R^{PS} = -\alpha p \left[\left(\frac{\beta_0}{\alpha_0} + \frac{1}{2}\right)\frac{\delta\rho}{\rho} + 2\left(\frac{\beta_0}{\alpha_0}\right)\frac{\delta\beta_0}{\beta_0} \right] \quad (20)$$

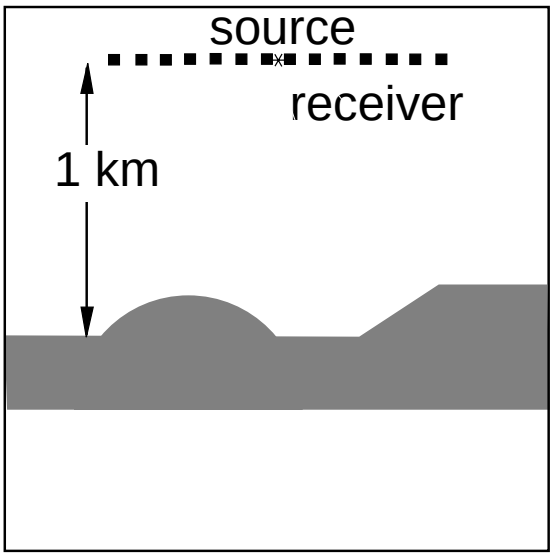

Figure 2: Two dimensional models used to compare the results from screen-approximation method and FD method. The model is a 2D profile from the French model. The parameters for the background medium is $V_P = 3.6km/s$, $V_S = 2.08km/s$ and $\rho = 2.2g/cm^3$. The intermediate layer has a -20% perturbation for both P- and S-wave velocities.

where $\rho_2\alpha_2 - \rho_1\alpha_1$ is the impedance contrast across the interface. Equations (19) and (20) are consistent with the reflectivities for waves near-vertically incident on a plane interface. Figure 1 gives acoustic reflectivities from different approximations including equations (17) and (19). The impedance contrast is 36%. The wide angle approximation gives good result for reflectivity vasus incident angle. In conclusion, for wide angle approximation, the accuracy of the reflectivity equivalent to reflection coefficients between two similar half-spaces. For small angle approximation, the reflectivity equivalent to reflection coefficient for nearly vertical incidence. If the amplitude-versus-incident-angle is an important issue, the wide angle version should be adopted. If one is mostly interested in amplitude linked with impedance contrast, the small angle version will give satisfactory results.

Accuracy of waveforms

In this section we will give some numerical simulations to show the accuracy of waveforms. The model is a 2D slice from the French model. Figure 2 shows the velocity structure of this model. The source and the receivers are located $1km$ above the upper interface. The synthetic seismograms are calculated using the elastic complex screen method. Small angle ap-

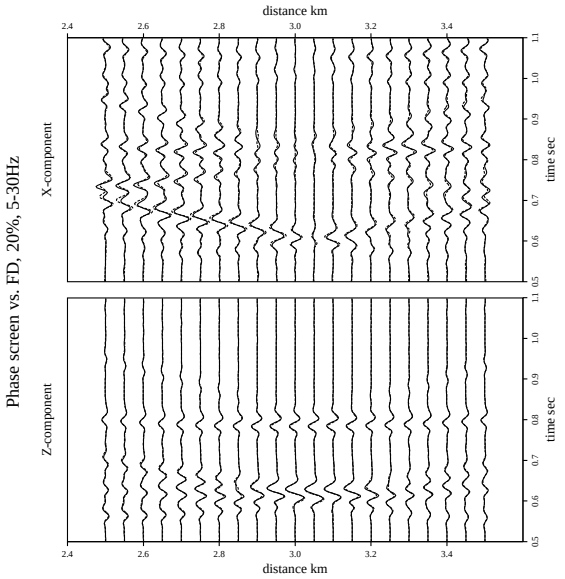

Figure 3: Comparison between results of 2D model from different methods. The solid lines are from screen method and the dash lines are from finite-difference method. The results show general agreement between the two methods in both amplitude and arrival times.

proximation (11)-(14) is used in the present calculation. The full wave 2D FD method is used to calculate synthetic seismograms for comparison. The free surface effects and direct arrivals have been properly removed from these results. The synthetic seismograms are basically reflections from the structure. The results are compared in Figure 3. Solid lines are from complex screen method and the dash lines are for that from FD method. For Z-component, there are mainly P-wave energy. Since the interface is rather complicated, there are several arrivals can be identified. The X-component of the synthetics is composed of P to S reflections from both interfaces as well as some P-wave energy. Generally speaking, the waveform agreement between the two methods is very good.

Conclusions

The elastic complex screen method is based on the one-way wave equation method. It provides an efficient way for propagating the wave field in both forward and backward directions. For wide angle approximation, the accuracy of the reflectivity equivalent to reflection coefficients under small velocity contrast. For small angle approximation, the reflectivity equivalent to reflection coefficient for nearly vertical incidence. Synthetic seismograms for 2D elastic models are generated based on small angle approximation. The resulted waveforms are compared with that from full FD method. For small to medium scattering angles, the method show good agreement with the FD method. For wide angle reflections, there are errors for both the phase and amplitude calculated by the small angle approximations, and suggesting that the wide angle approximation is required.

Acknowledgements

The support from the ACTI project of UCSC granted from the United States Department of Energy administrated by the Los Alamos National Laboratory and the facilities supported from the W.M. Keck Foundation are acknowledged.

References

Aki, K., and P.G. Richards, 1980, Quantitative Seismology: Theory and Methods, Vol. 1 and 2, W.H. Freeman, New York.

Martin, J.M., and Flatté, S.M., 1988, Intensity images and statistics from numerical simulation of wave propagation in 2-D random media: Appl. Opt., **17**, 2111-2126.

Stoffa, P.L., Fokkema, J.T., Freire, R.M.D. and Kessinger, W.P., 1990, Split-step Fourier Migration: Geophysics, **55**, 410-421.

Wu, R.S., 1994, Wide-angle elastic wave one-way propagation in heterogeneous media and an elastic wave complex-screen method: J. Geophys. Res., **99**, 751-766.

Wu, R.S., 1996, Synthetic seismograms in heterogeneous media by one-return approximation, Pure and Applied Geophys., **148**, 155-173.

Wu, R.S., and Huang, L.J., 1995, Reflected wave modeling in heterogeneous acoustic media using the De Wolf approximation, in: Mathematical Methods in Geophysical Imaging III, SPIE Proceedings Series, **2571**, 176-193.

Wu, R.S., Huang, L.J. and Xie, X.B., 1995, Backscattered wave calculation using the De Wolf approximation and a phase-screen propagator: Expanded abstracts, SEG 65th Annual Meeting, 1293-1296

Wu, R.S. and X.B., Xie, 1994, Multi-screen backpropagator for fast 3D elastic prestack migration, in: Mathematical Methods in Geophysical Imaging II, SPIE Proceedings Series, **2301**, 181-193.

Xie, X.B. and Wu, R.S., 1995, A complex-screen method for modeling elastic wave reflections: Expanded abstracts, SEG 65th Annual Meeting 1269-1272.

Xie, X.B. and Wu, R.S., 1996, 3D elastic wave modeling using the complex screen method, Expanded abstracts, SEG 66th Annual Meeting, 1247-1250.